GaN Monolithic Bidirectional Switch: A Review

Fan Li, Shiqiang Wu, Ang Li, Yuhao Zhu, Huiqing Wen, Wen Liu*

Abstract—This article systematically reviews the roadmap of GaN-based monolithic bidirectional switches, which play a critical role in AC power conversion. Three different monolithic integration categories are summarized. The first category is GaN HEMT with embedded diode bridge; the second approach utilizes reverse conducting and blocking capabilities of GaN devices; the third approach takes advantage of the unique feature of GaN HEMT to create a dual-gate bidirectional switch. Moreover, the variations based on the dual-gate structure are also thoroughly considered. The device parameters of the abovementioned methods have been analyzed, and the on-state energy loss has been evaluated. The commercial GaN-based bidirectional switches have also been compared with silicon-based counterparts, showing higher operation voltage, lower on-state resistance, and higher current capability. This article presents a comprehensive review of the state-of-the-art GaN bidirectional switch technology, which will provide insight into the research and design.

Index Terms—GaN HEMT, Bidirectional Switch, Monolithic Integration, Power Device

I. Introduction

In recent years, the AlGaN/GaN High Mobility Transistor (HEMT) has turned out to be a promising wide band-gap semiconductor device. Due to the large band gap and the high critical electric field of GaN material, GaN HEMT can operate at high voltage levels with a large power density and a low on-resistance [1], [2]. Previous studies have investigated the application potential of GaN devices under high-temperature environments [3]–[5]. The high thermal conductivity of GaN can improve the heat dissipating ability, which is beneficial to reduce the heat sinks [6]. These superior features could enhance device efficiency while reducing overall size, making GaN devices ideal for power conversion applications. Therefore, GaN-based power switches have been thoroughly studied and vastly adopted across various fields, such as DC-DC buck converters [7]–[9]. In recent years, GaN bidirectional switches have also begun to attract extensive research interest. With the lateral structure, AlGaN/GaN HEMT utilizes the 2DEG channel and avoids the body diode thus facilitating the switching applications, for those that require bidirectional conducting and bidirectional blocking capabilities. Expected features of such devices include a fast switching speed, a high blocking voltage, a low on-resistance, and a low voltage offset (V_{on}).

TABLE I
Different methodologies for bidirectional switches.

Approach	Advantage	Disadvantage
Si MOSFET	Low Voltage Offset	Low Voltage Tolerance
Si IGBT	High Power / Voltage	Body Effect Parasitics / Losses Large On-resistance
SiC MOSFET	High Power / Voltage	Expensive Body Effect
GaN HEMT	No Body Effect Small Chip Area High Switching Speed	Relative Expensive

There are several methods to realize a bidirectional switch through discrete devices, such as Si-based Metal Oxide Semiconductor Field effect transistors (MOSFET), Insulated Gate Bipolar Transistors (IGBT)) and SiC MOSFET. As illustrated in Table I, the Silicon-based MOSFET, IGBT, SiC MOSFET, and GaN HEMT approaches possess their respective advantages and disadvantages [10]. Among the abovementioned methods, IGBTs play a pivotal role, where the bidirectional switch topology consists of two anti-parallel IGBTs and two blocking diodes [11]. At least four discrete devices are needed to realize the function. Such device configuration results in a lengthy current path, increased parasitic parameters, and a high V_{on}. Moreover, the series connection of two unidirectional power devices increases conduction losses and doubles the total on-resistance compared to a monolithic bidirectional device. To overcome the shortcomings of discrete devices, there have been a number of researches that focus on the monolithic approach [12]–[14]. Driven by the pursuit of high efficiency and high power density, GaN-based bidirectional switching devices are obtained via monolithic integration, which minimizes the size of switches and enhances system efficiency.

This paper gives a comprehensive review of the device structure and performance of a monolithic GaN-based bidirectional switch. Section II presents the three most common monolithic integrated methods of GaN bidirectional switch, they are GaN HEMT embedded with diode bridge, reverse conduction and blocking bidirectional GaN

This work was supported by the National Key R&D Program of China (2022YFB3604400), the Suzhou Science and Technology program SYG202131, XJTLU Research Development Funding RDF-20-02-43. (Corresponding author: Wen Liu.)

Fan Li and Shiqiang Wu contributed equally to this work and should be considered co-first authors.

Fan Li, Ang Li and Yuhao Zhu are with the Department of Electrical Engineering and Electronics, University of Liverpool, Liverpool L69 3GJ, UK; Fan Li, Shiqiang Wu, Huiqing Wen, and Wen Liu are with the School of Advanced Technology, Xi'an Jiaotong-Liverpool University, Suzhou 215123, China.

HEMTs, and dual gate devices. Section III compares the three different types of GaN bidirectional switches' device-level parameters, on-state energy losses, and different application scenarios. Lastly, the comparisons between the monolithic GaN bidirectional switch product and its silicon counterparts are summarized.

II. Topologies of GaN Bidirectional Switches

The bidirectional switches obtained via monolithic integration have been classified into three categories based on the device topology. To prevent damage under faulty device turn-on and circuit failure, all the reviewed bidirectional switches are Enhancement mode (E-mode) or normally-off devices. The E-mode operation could be achieved using recessed-gate metal-insulator-semiconductor high-electron-mobility transistor (MIS-HEMT) or p-type gallium nitride (p-GaN) gate structures. The complexity of the device structures and their corresponding driver control designs have also been discussed in this section.

A. GaN HEMT with Embedded Diode Bridge

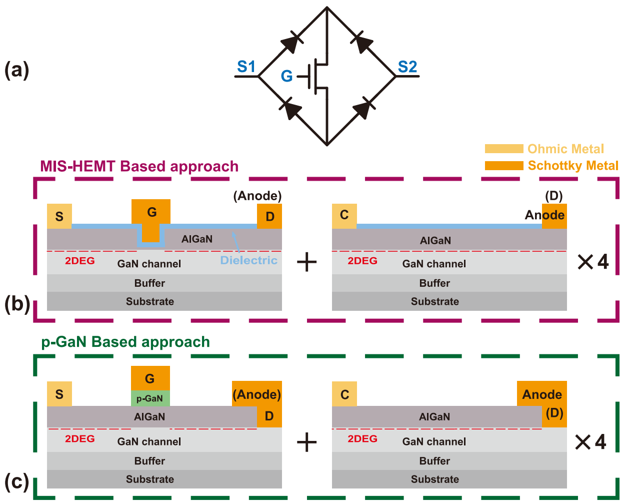

Fig. 1. (a) Equivalent circuit diagram, and the cross-section view of the embedded diode bridge bidirectional switches with (b) recessed gate MIS-HEMT structure [12] and (c) p-GaN gate structure [13].

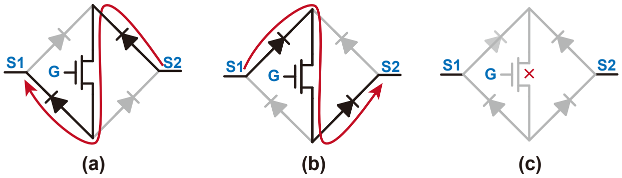

Fig. 2. The operation principle of embedded diode bridge structure [12]. (a) Reverse turn-on mode. (b) Forward turn-on mode. (c) Off mode.

Fig. 1 demonstrates the GaN bidirectional switch with a diode bridge structure comprising four SBDs and one HEMT. The bidirectional switches incorporate monolithic integrated Schottky barrier diodes (SBDs), which can be implemented through both recessed gate MIS-HEMTs [12] and p-GaN gate approaches [13]. The devices on the commercial p-GaN platform exhibit superior threshold stability due to the elimination of the gate etching process from recessed gate MIS-HEMT fabrication. Specifically, with the series connection of the diode, HEMT, and diode, the cathode of the first diode can be combined with the source electrode of the HEMT. As a result, the diode bridge topology has been further simplified. Fig. 2 illustrates the forward and reverse conduction current paths. This structure requires only one gate control hence employing a relatively simple driver design. However, the current still needs to pass through two SBDs and one HEMT during the conduction, which causes a relatively high offset voltage V_{on} that may degrade the conduction efficiency.

B. GaN HEMT with Reverse Conducting/Blocking Capabilities

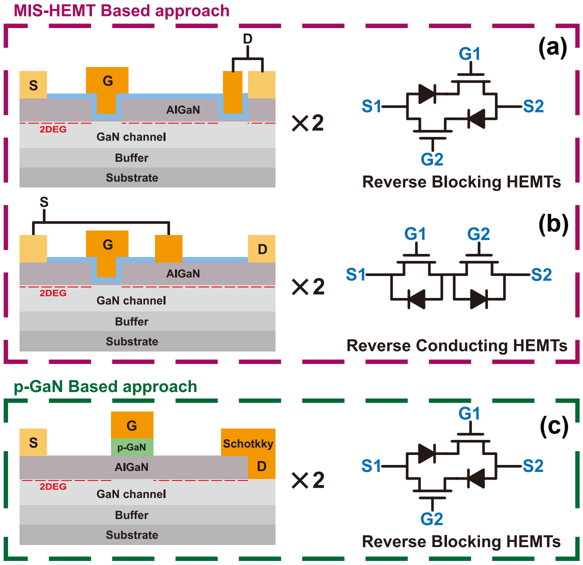

Fig. 3. The reverse blocking/reverse conducting HEMT (RB/RC-HEMT) based bidirectional switch. The cross-section view and equivalent circuit diagram of (a) MIS-HEMT based RB-HEMT [14], (b) MIS-HEMT based RC-HEMT [15] and (c) p-GaN gate HEMT based RB-HEMT [16].

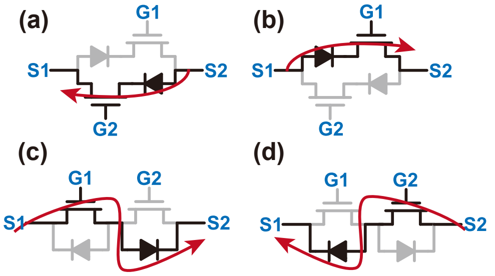

Fig. 4. The operation principle of (a) (b) RB-HEMT and (c) (d) RC-HEMT.

In AC-related applications, the reverse blocking capability for bidirectional switches is essential. Two anti-parallel GaN HEMTs with reverse blocking capabilities can be utilized as the bidirectional switch. The objective of design lies in the trade-off among a high reverse blocking voltage, a low V_{on}, and a low R_{on}. Extensive research has been focused on the engineering of the drain nodes to improve the reverse blocking capability [17], [18]. Fig. 3 (a) shows the GaN bidirectional switch that adopts a MIS Field Effect Drain (MIS-FED) architecture in place of the conventional drain electrode. This MIS-FED integrates the MIS structure into the drain area, allowing the device to conduct only when the drain area is at a voltage that can recover the 2DEG channel underneath the MIS-FED. Fig. 3 (c) demonstrates the widely adopted Schottky drain structure based on p-GaN HEMTs.

Nevertheless, the reverse blocking configuration in a bidirectional switch will bring the offset voltage V_{on} that reduces the conduction efficiency. Consequently, an alternative bidirectional switch architecture that utilizes the reverse conducting mechanism has been developed. As shown in Fig. 3 (b), the reverse conducting MIS-HEMT (RC-MISHEMT) employs the SBD structure located between the Schottky electrode and the AlGaN layer. As a result, this structure corresponds to a MIS-HEMT in parallel with an SBD that is turned on for reverse conduction, and a complete bidirectional switch function comprises a reverse series connection of two such devices [14] [15].

The operational principles of RB-HEMT and RC-HEMT as bidirectional switches are illustrated in Fig. 4, respectively. When one of the two gates is connected to a voltage below the threshold voltage (V_{th}), the current path in this direction is shut. Furthermore, when both gates are connected to voltages below V_{th}, the device enters the off state. And a maximum breakdown voltage in [16] could achieve 664 V and -651 V.

C. Dual Gate GaN Bidirectional Switch

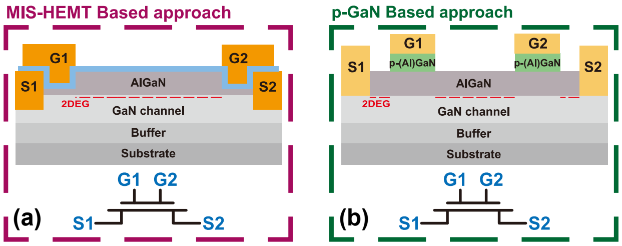

Fig. 5. The cross-section view and equivalent circuit diagram of Dual gate GaN bidirectional switch (a) MIS-HEMT [19] and (b) p-GaN gate [20], [21].

The third category of the bidirectional switch consists of a single device with a dual gate structure. Unlike the first two types of bidirectional switches, the third type can achieve a complete bidirectional switching function using a single device. As shown in Fig. 5 and Fig. 6, this type of bidirectional switch has garnered significant attention in AC applications.

TABLE II

OPERATION PRINCIPLE FOR DUAL GATE BIDIRECTIONAL SWITCH [20]

V_{G1S1}	V_{G2S2}	Mode
OFF	OFF	OFF-State
ON	ON	ON-State
ON	OFF	Diode Mode
OFF	ON	Diode Mode

Fig. 5 (a) and (b) illustrate devices with a dual gate structure of common drain configuration. Although their gate structures are different, the equivalent device structure diagrams are identical. The control signals on each gate need to be relative to the correspondent source signal. Fig. 5 (a) [19] utilizes the MIS structure with a recessed gate to deplete the 2DEG [22]. Meanwhile, Fig. 5 (b) employs the p(Al)GaN gate structure to deplete the 2DEG [21]. Morita et al. first present the development of a bidirectional switch using p-GaN Gate injection transistor (GIT) technology [20]. The operation principle for the GaN dual gate device is summarized in the TABLE II. Guacci et al. further explain the principles of the p-GaN GIT dual gate bidirectional switch using an equivalent circuit diagram [23]. Moreover, Ueno et al. [24] investigate the effect of substrate termination during on-state operation.

Apart from the abovementioned primary dual gate GaN bidirectional switches, this structure has been further improved by researchers. He et al. [25] proposes a dual gate structure with a field plate structure. To improve the breakdown voltage, the device size and chip size have been reduced, and the parasitic effects and the system efficiency and reliability have been improved. Furthermore, Zhao et al. [26] introduce a bidirectional switching device that has substrate potential management capability. This device consists of a control node, a first power/load node, a second power/load node, and a primary substrate and incorporates a nitride-based bi-lateral transistor. A substrate potential management circuit is implemented to regulate the potential of such a primary substrate. The resulting device can maintain a stable substrate potential in both directions when conducting current.

1) Self-Reverse-Blocking Dual-gate Bidirectional Switch: Apart from Fig. 5 (a) and (b), the dual gate device can also be in the depletion mode (D-mode) [27]. Despite its similar dual gates and substrate structure, it is not widely used due to its negative threshold voltage. Nevertheless, the current collapse test conducted on the D-mode dual gate device can still provide valuable insights for the design of bidirectional switches. Fig. 6 presents a variation to such as dual gate structures. Specifically, it builds upon Fig. 5 (b) by integrating a Si-based low-voltage Schottky diode between ”G2” and ”S2”. This design allows for implementing a self-reverse-blocking function without introducing additional complexity to the driver design [28].

2) Common Source/Drain GaN Bidirectional Switch: Fig. 7 (a) incorporates a reference voltage node in the common drain area. This modification transforms the device from a 4-terminal to a 5-terminal device, which evolves different control and operation techniques for specific converter

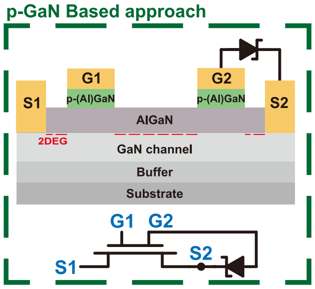

Fig. 6. The cross-section view of self-reverse-blocking dual-gate bidirectional switch with Si-based Schottky diode [28].

applications [29]. The Fig. 8 demonstrates the layout for the abovementioned dual-gate structures. It can be seen that for the same voltage-blocking capability, the common drain/source structure will increase the device area due to the symmetrical drift region for both sides. Consequently, the most compact design should eliminate the middle reference node so that the common access region can be shared.

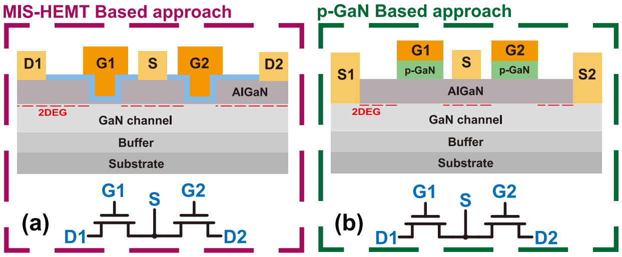

Fig. 7. The common source bidirectional structure with source electrode in the middle, the E-mode operation is realized by (a) recessed gate MIS-HEMT structure [30] and (b) p-GaN gate structure.

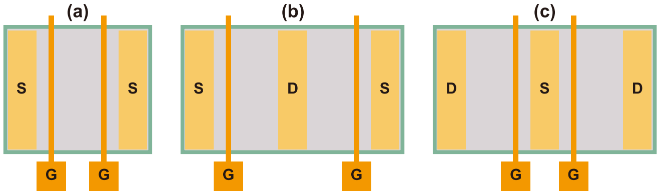

Fig. 8. The device layout for (a) dual gate, (b) common drain and (c) common source topologies for GaN bidirectional switch.

For the driver design of dual gate GaN bidirectional switch, Fig. 9 distinguishes the differences in the driver control for the dual-gate bidirectional switch and its variations. The floating driver ICs are connected to respective source nodes and need to be isolated. Nagai et al. [31], [32] propose an isolated Drive-by-Microwave gate driving module for the dual-gate bidirectional switch. The driver provides isolated gate power and signals through 2.4 GHz microwave wireless power transmission. It also incorporates a self-closing signal output rectifier that maintains low power consumption even at high switching frequencies. With two PWM signal inputs, the driver can effectively control the two gates of the devices. The driver also features low power consumption, high speed, fast propagation delay, and large common-mode suppression, making it very suitable for driving high-speed power devices in bidirectional switch applications.

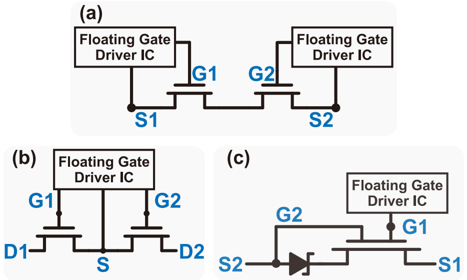

Fig. 9. The device layout for (a) dual gate, (b) common drain/source, and (c) self-reverse-blocking bidirectional switch.

III. Performance Analysis of the GaN Bidirectional Switch

A. Device Level Parameters and On-state Energy Loss Analysis

Table III presents a comparison of device parameters for bidirectional switches, including implementation, on-state offset voltage (V_{on}), threshold voltage (V_{th}), breakdown voltage (BV), on-state resistance (R_{on}), maximum load current ($I_{d,max}$), and reverse leakage current. The structure described in [12] exhibits the best BV capability among the listed devices. The increased distance between the drain and gate, effectively lowers the electric field between the common drain region, enabling the device to withstand higher voltage. As a result, it exhibits superior breakdown voltage compared to the double gate devices described in [20] [21].

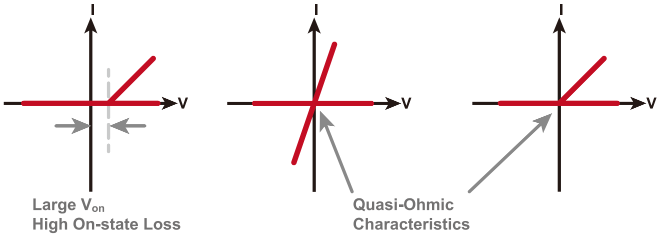

Fig. 10. V-I characteristics of (a) the bipolar voltage blocking and unidirectional current conduction, with a large $\boldsymbol{V_{on}}$. (b) bidirectional conduction capability that has a quasi-ohmic (small $\boldsymbol{V_{on}}$) feature, (c) integrated active synchronous rectification with quasi-ohmic feature.

In the previous section, three types of bidirectional switches are discussed, and it is essential to assess their on-state energy consumption [34] by considering its on-state offset voltage (V_{on}). From Ueno et al. [24], the reduction of the V_{on} could reduce the on-state resistance which further cut down the on-state energy loss. This means the on-state resistance R_{on} is positively correlated to on-state offset voltage V_{on} [35]. In the case of conduction, for an embedded diode bridge bidirectional switch, the V_{on} is the sum of the on-state offset voltage of two cascaded diodes, corresponding to 0.56 V * 2 [13]. For reverse-blocking bidirectional switches (Fig. 3 (a)) and reverse

TABLE III
THE DETAILED DEVICE PARAMETERS OF THE REVIEWED GAN MONOLITHIC BIDIRECTIONAL SWITCHES.

Reference	Method	V_{on} (V)	V_{th} (V)	BV (V)	$R_{on}/R_{on,sp}$	$I_{d,max}$ (mA/mm)	Reverse leak current (mA/mm)
Diode Bridge							
2015 [13]	MIS-HEMT	1.12	1	861/-946	/	120 (V_G = 12 V)	/
2021 [12]	p-GaN	1.13	1.84	1105/-1115	/	140 (V_G = 7 V)	$1.6e^{-4}$ (V_{ds} = -100 V)
Reverse Conducting/Blocking							
2017 [14]	TCAD	0.38	4.1 (5 A)	950/-900 (10 μA)	/	/	/
2017 [15]	TCAD	0	7.6 (5 A)	500/-500 (100 μA)	/	/	/
2021 [16]	p-GaN	0.63	1.85	664/-651 (1 μA/mm)	30 Ω*mm	225 (V_G = 7 V)	$1e^{-4}$
Dual Gate							
2007 [20]	GIT	1.5	1	650	3.1 mΩ*cm^2	/	/
2017 [19]	TCAD MIS	3.55	/	500/-500	/	1200 (V_G = 10 V)	/
2018 [21]	GIT	1.5	0.5	900/-900	2.5 mΩ*cm^2	/	/
2022 [33]	D-mode	/	-3.6	1129/1063	/	475 /375	$1e^{-4}$

conducting bidirectional switches (Fig. 3 (b)), the V_{on} is determined by the turn-on voltage of a single diode. For example, the V_{on} of reverse-blocking bidirectional switches is 0.38 V [14], while the V_{on} of reverse conducting bidirectional switches is 0.63 V [16]. It is worth noting that in [14], the V_{on} of reverse-blocking bidirectional switches tends to be slightly lower than that of reverse conducting switches. Regarding dual gate bidirectional switches, the V_{on} is typically determined by the voltage required for unidirectional circuits to conduct [35], and it is commonly observed when one gate is on while the other gate is off to exhibit diode characteristics. The V_{on} of dual gate bidirectional switches ranges from 1.5 V in [20] and [21] to 3.5 V in [19], which also strongly correlates with the fabrication process. As for the dual gate device with reference gate voltage, its V_{on} is generally similar to that of a device without a reference voltage; however, process optimization can reduce it to 0.35 V [30].

B. GaN Bidirectional Switch for AC Applications

In a conventional DC-AC conversion system, the T-type inverter is responsible for bidirectional operation. This is an extension of the half-bridge topology [21], as illustrated in Fig. 11 (a). Nonetheless, T-type inverters have several notable issues, such as high conduction loss and parasitic effects, which lead to slow switching speed and substantial voltage oscillations during switching transitions [36].

With regard to AC-AC conversion systems, The voltage level of the bidirectional switch is the main determinant of the upper power limit of the matrix converter, and the switching loss of the bidirectional device is the vital factor for the efficiency of the matrix converter [37] [38]. Therefore, with high-voltage blocking capability, fast switching speed, and high conversion efficiency [39], applying GaN bidirectional switches to AC-AC matrix converters could reduce the total cost and size of the system [14] [16] [40], [41].

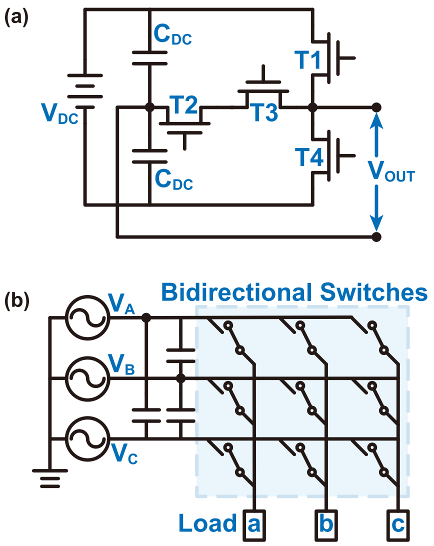

Fig. 11. (a) T-type inverter topology, which is an implementation of bidirectional switch [21]. (b) The AC-AC matrix converter with bidirectional switch array [42].

In Fig. 11 (b), matrix converters generate output voltages with different amplitudes and frequencies by controlling the duty cycle of bidirectional switches [42] [37]. the bidirectional switch array is the primary power element to create a variable output voltage system at the desired frequencies. [42]. The AC-AC power conversion system can find vast applications, especially in motor drives. The increased interest in power efficiency accelerates the research of AC-AC matrix converters. The loss and power capability are the critical factors for the system's efficiency, which could benefit from the advantages of GaN bidirectional switches. For example, the AC-AC conversion in a three-phase matrix converter combines the generation and motoring function with a set of nine bidirectional switches. It eliminates the need for energy storage components in the DC link and enhances system efficiency and reliability [40]. It has also been applied in fast charging and energy feedback to the grid in electric vehicle charging. The device can find further applications in solid-state circuit breakers to enhance system safety and reliability [41] [43].

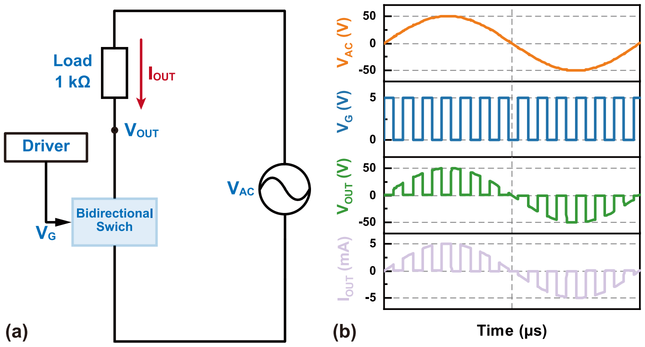

Fig. 12. (a) The circuit diagram for AC chopping test for the bidirectional switch. (b) The desired waveforms for the AC chopping circuit.

In order to verify the functionality of the bidirectional switch, the AC chopping test in Fig. 12 (a) is the most common measurement setup. one or more driver signals V_G will be applied periodically to the DUT depending on the bidirectional switch topology. Fig. 12 (b) demonstrates the desired output waveforms for the AC chopper. The DUT should block the voltage and current for both polarities; such implementation can be found in numerous reports that are summarized in Table IV.

Table IV comprehensively compares the operating scenarios and relevant parameters for five published GaN bidirectional switches in AC/AC converters. Shi et al. [44] demonstrated the highest peak-to-peak input voltage amplitude of ± 200 V for the GaN bidirectional switch, indicating its high breakdown voltage. This characteristic makes the bidirectional switch suitable for AC/AC frequency conversion in high-voltage and multi-frequency applications. Furthermore, the bidirectional switch achieved a conversion efficiency of 90.5% at a low power level of 250 W and exceeded 98% at a high power level of 1 kW. Another noteworthy achievement was reported by Wang et al. [12], which indicates that an input signal of 60 Hz is converted to an output signal of 5 kHz, which meets the demand for AC-AC matrix converter applications.

C. The Comparison with Silicon counterparts

Table V primarily compares the product parameters of commercial GaN-on-Si and Si-based bidirectional switches. It can be observed that commercial GaN-on-Si bidirectional switch devices possess certain advantages over pure Si-based bidirectional switch devices, specifically in terms of high load current, high drain-to-source voltage, and low on-state resistance. Notably, the commercial GaN bidirectional switch device presented in [45] demonstrated a peak drain-to-source current of 20 A, which surpasses the best-performing Si-based device in Table V [50] that exhibited 7 A. Moreover, the V_{ds} max in [46], [47] is as high as 120 V, which is superior to the best-performing Si-based bidirectional switch [49] with 32 V. Additionally, the on-state resistance recorded in [45] was as low as 4 mΩ, representing a significant improvement compared to other Si-based bidirectional switch devices. These results illustrate that a commercial GaN bidirectional switch is capable of tolerating higher input voltages and currents while reducing losses through low on-state resistance. Lots of patents [54]–[58] for GaN bidirectional switches have been published, which implies that plenty of GaN bidirectional switch products will be commercialized.

IV. CONCLUSION

In conclusion, this review article analyzes and compares three different monolithic bidirectional switch designs based on GaN technology. Each design's structural characteristics, operating principles, and device performance parameters are thoroughly discussed. The results provide valuable insights and guidance for the development and selection of GaN-based bidirectional switches. Furthermore, a comparison between GaN-based and Si-based bidirectional switches is presented to demonstrate the exponential advantages of GaN technology in terms of on-resistance. This review summarizes the monolithic GaN-based bidirectional switch from the device's point of view to provide guidance in power electronics applications.

ACKNOWLEDGMENT

This work was supported by the National Key R&D Program of China (2022YFB3604400), the Suzhou Science and Technology program SYG202131, XJTLU Research Development Funding RDF-20-02-43.

REFERENCES

[1] M. Meneghini, C. De Santi, I. Abid, M. Buffolo, M. Cioni, R. A. Khadar, L. Nela, N. Zagni, A. Chini, F. Medjdoub, G. Meneghesso, G. Verzellesi, E. Zanoni, and E. Matioli, "GaN-based power devices: Physics, reliability, and perspectives," Journal of Applied Physics, vol. 130, no. 18, p. 181101, Nov. 2021.
[2] D. Kinzer, "GaN power IC technology: Past, present, and future," in 2017 29th International Symposium on Power Semiconductor Devices and IC's (ISPSD), May 2017, pp. 19–24, iSSN: 1946-0201.
[3] A. Li, M. Cui, Y. Shen, Z. Li, W. Liu, I. Z. Mitrovic, H. Wen, and C. Zhao, "Monolithic Comparator and Sawtooth Generator of AlGaN/GaN MIS-HEMTs With Threshold Voltage Modulation for High-Temperature Applications," IEEE Transactions on Electron Devices, vol. 68, no. 6, pp. 2673–2679, Jun. 2021.
[4] A. Li, Y. Shen, Z. Li, Y. Zhao, I. Z. Mitrovic, H. Wen, S. Lam, and W. Liu, "A Monolithically Integrated 2-Transistor Voltage Reference With a Wide Temperature Range Based on AlGaN/GaN Technology," IEEE Electron Device Letters, vol. 43, no. 3, pp. 362–365, Mar. 2022.

TABLE IV

The applications of the bidirectional switch as an AC switch.

Reference	AC Frequency (Hz)	AC Voltage (V)	Gate Frequency (Hz)	Gate Voltage (V)	Topology of bidirectional switch	Efficiency
2007 [20]	60	± 141	2 k	(0, 5)	Dual gate	97.5% (Three Phase Matrix)
2015 [13]	60	± 100	1 k	(0, 8)	Embedded diode bridge	/
2018 [44]	50	± 200	/	/	Dual gate	90.5%(250 W) 98%(1 kW) Three Phase Matrix
2021 [12]	60	± 150	5 k	(0, 5)	Embedded diode bridge	/
2021 [16]	60	± 100	2 k	(0, 5)	RB-HEMT	/

TABLE V

The comparisons of reviewed commercial GaN/Si bidirectional switch parameters.

Product	V_{ds}max(V)	R_{dson}(mΩ)	R_{dson} max (mΩ)	I_d max (A)	I_d pulse max (A)
			GaN-on-Si products		
[45]	40	4	4.8	20	100
[46]	120	80	110	3.4	20
[47]	120	40	58	5	20
			Si products		
[48]	2.85	30	40	1.83	/
[49]	32	62	/	1.5	/
[50]	5.5	7	10	7	/
[51]	6	950	1150	0.2	0.4
[52]	3.6	450	600	0.3	0.5
[53]	2	/	180	4	/

[5] A. Li, Y. Shen, Z. Li, F. Li, R. Sun, I. Z. Mitrovic, H. Wen, S. Lam, and W. Liu, “A 4-Transistor Monolithic Solution to Highly Linear On-Chip Temperature Sensing in GaN Power Integrated Circuits,” IEEE Electron Device Letters, vol. 44, no. 2, pp. 333–336, Feb. 2023.

[6] J. Millan, P. Godignon, X. Perpina, A. Perez-Tomas, and J. Rebollo, “A Survey of Wide Bandgap Power Semiconductor Devices,” Ieee Transactions on Power Electronics, vol. 29, no. 5, pp. 2155–2163, May 2014.

[7] M. Cui, R. Z. Sun, Q. L. Bu, W. Liu, H. Q. Wen, A. Li, Y. Liang, and C. Z. Zhao, “Monolithic GaN Half-Bridge Stages With Integrated Gate Drivers for High Temperature DC-DC Buck Converters,” Ieee Access, vol. 7, pp. 184 375–184 384, 2019.

[8] M. Cui, Q. Bu, Y. Cai, R. Sun, W. Liu, H. Wen, S. Lam, Y. C. Liang, I. Z. Mitrovic, S. Taylor, P. R. Chalker, and C. Zhao, “Monolithic integration design of GaN-based power chip including gate driver for high-temperature DC–DC converters,” Japanese Journal of Applied Physics, vol. 58, no. 5, p. 056505, May 2019.

[9] R. Sun, Y. C. Liang, Y.-C. Yeo, C. Zhao, W. Chen, and B. Zhang, “Development of GaN Power IC Platform and All GaN DC-DC Buck Converter IC,” in 2019 31st International Symposium on Power Semiconductor Devices and ICs (ISPSD). Shanghai, China: IEEE, May 2019, pp. 271–274.

[10] J. Yao, “Working principle and characteristic analysis of SiC MOSFET,” Journal of Physics: Conference Series, vol. 2435, no. 1, p. 012022, 2023.

[11] S. Chowdhury, C. W. Hitchcock, Z. Stum, R. P. Dahal, I. B. Bhat, and T. P. Chow, “Operating Principles, Design Considerations, and Experimental Characteristics of High-Voltage 4H-SiC Bidirectional IGBTs,” IEEE Transactions on Electron Devices, vol. 64, no. 3, pp. 888–896, Mar. 2017, conference Name: IEEE Transactions on Electron Devices.

[12] H. Y. Wang, W. Mao, C. Yang, S. L. Zhao, M. Du, X. F. Wang, X. F. Zheng, C. Wang, C. F. Zhang, J. C. Zhang, and Y. Hao, “High performance GaN-based monolithic bidirectional switch using diode bridges,” Applied Physics Express, vol. 14, no. 9, p. 5, Sep. 2021.

[13] B. R. Park, S. W. Han, and H. Y. Cha, “Diode Bridge Embedded AlGaN/GaN Bidirectional Switch,” IEEE Electron Device Letters, vol. 36, no. 4, pp. 324–326, Apr. 2015.

[14] Y. Shi, W. Chen, C. Liu, G. Hu, J. Liu, X. Cui, H. Tao, J. Zhang, Y. Shi, A. Zhang, Z. Li, Q. Zhou, and B. Zhang, “A high-performance GaN E-mode reverse blocking MISHEMT with MIS field effect drain for bidirectional switch,” in 2017 29th International Symposium on Power Semiconductor Devices and IC’s (ISPSD), May 2017, pp. 207–210, iSSN: 1946-0201.

[15] Y. Shi, W. Chen, F. Wang, J. Liu, X. Cui, G. Hu, C. Liu, Z. Li, Q. Zhou, and B. Zhang, “A GaN enhancement-mode reverse blocking MISHEMT with MIS field-effect drain for bidirectional switch,” Journal of Computational Electronics, vol. 17, no. 1, pp. 238–245, 2017.

[16] H. Wang, W. Mao, J. Luo, C. Yang, J. Chen, S. Zhao, M. Du, X. Zheng, C. Wang, C. Zhang, J. Zhang, and Y. Hao, “Experimental Demonstration of Monolithic Bidirectional Switch With Anti-Paralleled Reverse Blocking p-GaN HEMTs,” IEEE

Electron Device Letters, vol. 42, no. 9, pp. 1264–1267, Sep. 2021.

[17] R. Sun, F. Wang, P. Luo, W. Xu, Y. Wang, C. Liu, W. Chen, and B. Zhang, "High-performance Reverse Blocking p-GaN HEMTs with Multi-column p-GaN/Schottky Alternate-island Drain," in 2022 IEEE 34th International Symposium on Power Semiconductor Devices and ICs (ISPSD), May 2022, pp. 173–176, iSSN: 1946-0201.

[18] C. Zhou, W. Chen, E. L. Piner, and K. J. Chen, "Schottky-ohmic drain algan/gan normally off hemt with reverse drain blocking capability," IEEE Electron Device Letters, vol. 31, no. 7, pp. 668–670, 2010.

[19] Y. Shi, W. Chen, Q. Zhou, and B. Zhang, "A non-Ohmic normally-off GaN monolithic bidirectional switch with MIS field effect schottky tunnel junction," Superlattices and Microstructures, vol. 109, pp. 414–422, Sep. 2017.

[20] T. Morita, M. Yanagihara, H. Ishida, M. Hikita, K. Kaibara, H. Matsuo, Y. Uemoto, T. Ueda, T. Tanaka, and D. Ueda, "650 V 3.1 mΩcm2 GaN-based monolithic bidirectional switch using normally-off gate injection transistor," in 2007 IEEE International Electron Devices Meeting, Dec. 2007, pp. 865–868, iSSN: 2156-017X.

[21] C. Kuring, O. Hilt, J. Bocker, M. Wolf, S. Dieckerhoff, and J. Wurfl, "Novel monolithically integrated bidirectional GaN HEMT," in 2018 IEEE Energy Conversion Congress and Exposition (ECCE). Portland, OR, USA: IEEE, Sep. 2018, pp. 876–883.

[22] M. Liu, H. Sun, X. Lin, and J. Chen, "Bidirectional switching transistor," China, Patent CN107154430B, Sep. 2017.

[23] M. Guacci, D. Zhang, M. Tatic, D. Bortis, J. W. Kolar, Y. Kinoshita, and H. Ishida, "Three-Phase Two-Third-PWM Buck-Boost Current Source Inverter System Employing Dual-Gate Monolithic Bidirectional GaN e-FETs," CPSS Transactions on Power Electronics and Applications, vol. 4, no. 4, 2019.

[24] H. Ueno, Y. Kinoshita, Y. Yamada, A. Suzuki, T. Ichiryu, M. Nomura, H. Fujiwara, H. Ishida, and T. Hatsuda, "A 3-Phase T-type 3-Level Inverter using GaN Bidirectional Switch with Very Low On-State Resistance," p. 4, 2019.

[25] J. He, Z. Lin, Y. Lin, C. Liu, N. Xu, Y. Fang, and N. Ye, "Gallium nitride bidirectional switching device and preparation method," China, Patent CN113903798A, Jan. 2022.

[26] J. Zhao, C. Zhou, M. Li, W. Gao, C. Yang, G. Yang, and S. Cheng, "Nitride based semiconductor bidirectional switching device and manufacturing method," China, Patent CN115117055A, Sep. 2022.

[27] Y. Kudoh, K. Mizutani, N. Otsuka, D. Ueda, S. Takahashi, M. Inamori, H. Yamagiwa, T. Morita, T. Ueda, T. Tanaka, and T. Morizane, "Single to two-phase matrix converter using GaN-based monolithic bidirectional switch for driving symmetrical two-phase motor," in 2014 IEEE Energy Conversion Congress and Exposition (ECCE). Pittsburgh, PA, USA: IEEE, Sep. 2014, pp. 3186–3191.

[28] N. Nain, S. Walser, J. Huber, K. K. Leong, and J. W. Kolar, "Self-Reverse-Blocking Control of Dual-Gate Monolithic Bidirectional GaN Switch With Quasi-Ohmic on-State Characteristic," IEEE Transactions on Power Electronics, vol. 37, no. 9, pp. 10 091–10 094, Sep. 2022.

[29] S. Leo, F. Jean-Paul, F. David, J. Pierre-Olivier, P. Pierre, and L. Othman, "Implementation of monolithic bidirectional switches in a AC/DC Dual Active Bridge in ZVS auto-switching mode," in 2018 IEEE International Conference on Industrial Technology (ICIT). Lyon: IEEE, Feb. 2018, pp. 742–746.

[30] J. Waldron and T. P. Chow, "Physics-based analytical model for high-voltage bidirectional GaN transistors using lateral GaN power HEMT," in 2013 25th International Symposium on Power Semiconductor Devices & IC's (ISPSD). Kanazawa: IEEE, May 2013, pp. 213–216.

[31] S. Nagai, Y. Kawai, O. Tabata, S. Choe, N. Negoro, and T. Ueda, "A high-efficient driving isolated Drive-by-Microwave half-bridge gate driver for a GaN inverter," in 2016 IEEE Applied Power Electronics Conference and Exposition (APEC). Long Beach, CA, USA: IEEE, Mar. 2016, pp. 2051–2054.

[32] S. Nagai, Y. Yamada, N. Negoro, H. Handa, M. Hiraiwa, N. Otsuka, and D. Ueda, "A 3-Phase AC–AC Matrix Converter GaN Chipset With Drive-by-Microwave Technology," IEEE Journal of the Electron Devices Society, vol. 3, no. 1, pp. 7–14, Jan. 2015.

[33] D.-J. Lin, J.-Y. Yang, C.-K. Chang, and J.-J. Huang, "Study of Current Collapse Behaviors of Dual-Gate AlGaN/GaN HEMTs on Si," IEEE Journal of the Electron Devices Society, vol. 10, pp. 59–64, 2022.

[34] R. Hou, Y. Shen, H. Zhao, H. Hu, J. Lu, and T. Long, "Power Loss Characterization and Modeling for GaN-Based Hard-Switching Half-Bridges Considering Dynamic on-State Resistance," IEEE Transactions on Transportation Electrification, vol. 6, no. 2, pp. 540–553, 2020.

[35] O. C. Spro, D. Peftitsis, O.-M. Midtgard, and T. Undeland, "Modelling and quantification of power losses due to dynamic on-state resistance of GaN E-mode HEMT," in 2017 IEEE 18th Workshop on Control and Modeling for Power Electronics (COMPEL), 2017, pp. 1–6.

[36] C. L. Solanki, M. H. Ayalani, and S. Gohil, "Performance of Three Phase T-Type Multilevel Inverter with Reduced Switch Count," in 2018 International Conference on Current Trends towards Converging Technologies (ICCTCT), Mar. 2018, pp. 1–5.

[37] P. Wheeler, J. Rodriguez, J. Clare, L. Empringham, and A. Weinstein, "Matrix converters: a technology review," IEEE Transactions on Industrial Electronics, vol. 49, no. 2, pp. 276–288, Apr. 2002, conference Name: IEEE Transactions on Industrial Electronics.

[38] P. Szczesniak, J. Kaniewski, and M. Jarnut, "AC–AC power electronic converters without DC energy storage: A review," Energy Conversion and Management, p. 15, 2015.

[39] H. Wang, W. Mao, S. Zhao, B. Gao, M. Du, X. Zheng, C. Wang, C. Zhang, J. Zhang, and Y. Hao, "High-performance reverse blocking p-GaN HEMTs with recessed Schottky and p-GaN isolation blocks drain," Applied Physics Letters, vol. 119, no. 2, p. 023507, Jul. 2021, publisher: American Institute of Physics.

[40] J. Huber and J. W. Kolar, "Monolithic Bidirectional Power Transistors," IEEE Power Electronics Magazine, vol. 10, no. 1, pp. 28–38, Mar. 2023.

[41] T. Luan, Q. Jiang, S. Huang, X. Wang, H. Jin, F. Guo, Y. Yao, J. Fan, H. Yin, K. Wei, Y. Li, H. Jiang, J. Li, and X. Liu, "Investigation of trapping/de-trapping dynamics of surface states in AlGaN/GaN high-electron mobility transistors based on dual-gate structures," Microelectronic Engineering, vol. 269, p. 111916, Jan. 2023.

[42] H. Umeda, Y. Yamada, K. Asanuma, F. Kusama, Y. Kinoshita, H. Ueno, H. Ishida, T. Hatsuda, and T. Ueda, "High power 3-phase to 3-phase matrix converter using dual-gate GaN bidirectional switches," in 2018 IEEE Applied Power Electronics Conference and Exposition (APEC). San Antonio, TX, USA: IEEE, Mar. 2018, pp. 894–897.

[43] M. Guacci, M. Tatic, D. Bortis, J. W. Kolar, Y. Kinoshita, and H. Ishida, "Novel Three-Phase Two-Third-Modulated Buck-Boost Current Source Inverter System Employing Dual-Gate Monolithic Bidirectional GaN e-FETs," in 2019 IEEE 10th International Symposium on Power Electronics for Distributed Generation Systems (PEDG). Xi'an: IEEE, Jun. 2019, pp. 674–683.

[44] H. Umeda, Y. Yamada, K. Asanuma, F. Kusama, Y. Kinoshita, H. Ueno, H. Ishida, T. Hatsuda, and T. Ueda, "High power 3-phase to 3-phase matrix converter using dual-gate GaN bidirectional switches," in 2018 IEEE Applied Power Electronics Conference and Exposition (APEC). San Antonio, TX, USA: IEEE, Mar. 2018, pp. 894–897. [Online]. Available: http://ieeexplore.ieee.org/document/8341119/

[45] Innoscience, USA [Online]. Available: https://www.semiee.com/file/Innoscience/Innoscience-INN040W048A.pdf, Accessed on: Jun. 30, 2022.

[46] Efficient power conversion, USA [Online]. Available: https://epc-co.com/epc/Portals/0/epc/documents/datasheets/EPC2110_datasheet.pdf, Accessed on: Jun. 30, 2022.

[47] Efficient power conversion, USA [Online]. Available: https://epc-co.com/epc/Portals/0/epc/documents/datasheets/EPC2221_datasheet.pdf, Accessed on: Jun. 30, 2022.

[48] Microchip Technology, USA [Online]. Available: https://ww1.microchip.com/downloads/aemDocuments/documents/APID/ProductDocuments/DataSheets/UCS3205-Data-Sheet-DS20006433A.pdf, Accessed on: Jun. 30, 2022.

[49] NXP Semiconductors, Netherlands [Online]. Available: https:

//www.nxp.com/docs/en/data-sheet/NX5P3001.pdf, Accessed on: Jun. 30, 2022.
[50] Maxim Integrated, USA [Online]. Available: https://www.analog.com/media/en/technical-documentation/data-sheets/MAX14634-MAX14680.pdf, Accessed on: Jun. 30, 2022.
[51] On Semiconductor, USA [Online]. Available: https://www.onsemi.com/pdf/datasheet/fsa2257-d.pdf, Accessed on: Oct. 5, 2023.
[52] Texas Instruments, USA [Online]. Available: https://www.ti.com/lit/ds/symlink/ts3a5223.pdf?ts=1696483577744&ref_url=https253A252F252Fwww.ti.com252Fproduct252FTS3A5223, Accessed on: Jun. 30, 2022.
[53] STMicroelectronics, USA [Online]. Available: https://pdf1.alldatasheet.com/datasheet-pdf/view/447686/TGS/Z0409MF.html, Accessed on: Jun. 30, 2022.
[54] H. Liao and C. Zhou, “Gallium nitride semiconductor device with integrated continuous current diode,” China, Patent CN211529952U, Mar. 2020.
[55] J. Honea, P. Parikh, Y. Wu, and I. Ben-Yaacov, “Iii-nitride bidirectional switches,” USA, Patent US7875907B2, Jan. 2011.
[56] R. Baal, M. Skype, N. Peel, D. Anderson, and S. Pengdehacard, “Bidirectional gallium nitride switch and its forming method,” China, Patent CN104241282A, Dec. 2014.
[57] W.-C. Liao, J. Cao, R. Beach, Z. Tang, and E. Lee, “Bidirectional gan fet with single gate,” USA, Patent US2023/0111542A1, Apr. 2023.
[58] D. M. Kinzer and J. Zhang, “Bidirectional gan switch with built-in bias supply and integrated gate drivers,” USA, Patent US10651843B1, May 2020.